A Pseudo Plane-wave Gravitational Calibrator for Gravitational Wave Observatories

M.P. Ross,[1,*] J.H. Gundlach,[1] C. Weller,[1] E.G. Adelberger,[1] Jeff Kissel,[2]
Timesh Mistry,[3] Laurence Datrier,[4] Ed Daw,[3] and Martin Hendry[4]

[1] *Center for Experimental Nuclear Physics and Astrophysics, University of Washington, Seattle, Washington, 98195, USA*
[2] *LIGO Hanford Observatory, Richland, WA 99352, USA*
[3] *The University of Sheffield, Sheffield S10 2TN, UK*
[4] *SUPA, University of Glasgow, Glasgow G12 8QQ, UK*

The precision of existing gravitational calibrators are limited by their dependence on the relative position between the calibrators and the test masses. Here we present a novel geometry consisting of four quadrupole rotors placed at the vertices of a rectangle centered on the test mass. The phases and rotation directions are selected to produce a pseudo plane-wave sinusoidal gravitational acceleration with amplitude of 101.37 fm/s^2. This acceleration has minimal positioning dependence and can yield 0.15% acceleration amplitude uncertainty for 1 cm test mass positioning uncertainty. The acceleration is directed precisely along the optical axis of the interferometer arm and applies no torque on the test mass. In addition, the small size of the rotors has significant engineering and safety benefits.

I. INTRODUCTION

Gravitational wave astronomy has blossomed into a novel method to observe the universe. The number of gravitational wave observations is expected to grow substantially in the coming years with the continued operation of the LIGO [1] and Virgo [2] interferometers as well the future addition of LIGO-India [3] and the further improvements of KAGRA [4].

These interferometers must be precisely calibrated to accurately interpret gravitational wave signals. Whether for binary merger parameter estimation [5], cosmological measurements [6–8], or searches for deviations from general relativity [9], the strain readouts of the observatories must be precisely and accurately calibrated to yield accurate scientific results.

Currently, this calibration has been accomplished using photon pressure [10]. These versatile photon calibration systems have yielded absolute calibrations with $\sim 0.41\%$ uncertainty [11]. However, relying on a single calibration system can allow unknown systematics to skew the scientific results.

Calibrating with a gravitationally induced strain has long been suggested as an alternative calibration technique [12–17] and has recently been implemented at many of the gravitational wave observatories [18–21]. Operating both gravitational and photon calibration systems allows the systems to cross-check each other which increases the robustness of the astrophysical results. Additionally, the independent calibrations can be combined to yield a higher-precision combined absolute calibration.

Current single-rotor gravitational calibrators [18–21] produce accelerations that have large dependence on the radial distance, r, between the rotor and the test mass. The acceleration is typically proportional to $\sim 1/r^{l+2}$ where l is the order of the dominate mass-multipole moment. For example, a rotor with a quadrupole mass distribution ($l = 2$) will follow $\sim 1/r^4$. This strong positioning dependence causes the performance of the absolute calibration to be limited by the precision of the positioning measurements.

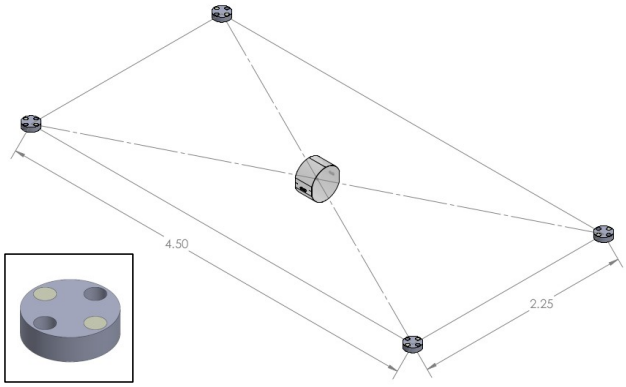

FIG. 1. A rendering of the geometry of the rotors with the test mass at the center of the 2.25-m by 4.50-m rectangle. Also shown is a detail of a single rotor consisting of the dark gray aluminum disk with two light gray tungsten slugs inserted into two of the four rotor holes.

Here, we present a novel geometry consisting of four quadrupole rotors that produces a pseudo plane-wave gravitational acceleration. This geometry produces an acceleration which has minimal first-order dependence on the position of the rotors allowing for improved calibration precision with limited positioning precision. Additionally, this geometry suppresses the torques acting on the test mass and eases much of the engineering and safety concerns of previous rotors.

* mpross2@uw.edu

Parameter	Mean	Uncertainty
Cylinder Mass	1 kg	0.3 g
Cylinder Radius	2 cm	2.5 μm
Cylinder Length	5 cm	5 μm
Quadrupole Radius	6 cm	5 μm
Test Mass	40 kg	10 g
Test Mass Length	200 mm	0.1 mm
Test Mass Radius	170 mm	0.05 mm
Test Mass Flat Width	327 mm	0.05 mm
Rotor Positions	($\pm$ 2.25 m, $\pm$ 1.125 m, 0 m)	(1 mm, 1 mm, 1 mm)
Test Mass Position	(0 m, 0 m, 0 m)	(1 mm, 1 mm, 1 mm)
Rotor Relative Phase	0°, 90°	1°

TABLE I. Parameters describing the rotors, the test mass, and their respective positions.

II. GEOMETRY

The pseudo plane-wave calibrator consists of four identical rotors placed at the vertices of a 2.25-m by 4.50-m rectangle centered on the test mass. Figure 1 shows a rendering of the geometry. The rotors are designed with the similar dimensions as the LIGO NCal [21] but without a hexapole mass arrangement. Each rotor is a 17-cm diameter, 5-cm tall aluminum disk with two holes cut at a radius of 6-cm separated by 90°. These holes are filled in with 4-cm diameter, 5-cm tall tungsten cylinders which produce a quadrupole mass distribution. The parameters of the geometry are displayed in Table I.

The rotor parameters that are common with the LIGO NCal are assigned uncertainties equal to what was previously achieved [21]. The rest of the parameters (positioning, phase, etc.) are assigned uncertainties based on what is reasonably achievable with standard measurement techniques. For example, since the rotors would be outside the interferometer's vacuum system, their positions can be readily measured to mm-precision with standard surveying equipment. [21]

The relative phases of the rotors and the rotation directions are set to achieve pseudo plane-wave nature. The four rotor with a positive x-coordinate are rotated by 90° from the rotors with negative x-coordinate. Additionally, the rotors with positive y-coordinate rotate clockwise while those with negative y-coordinates rotate counter-clockwise.

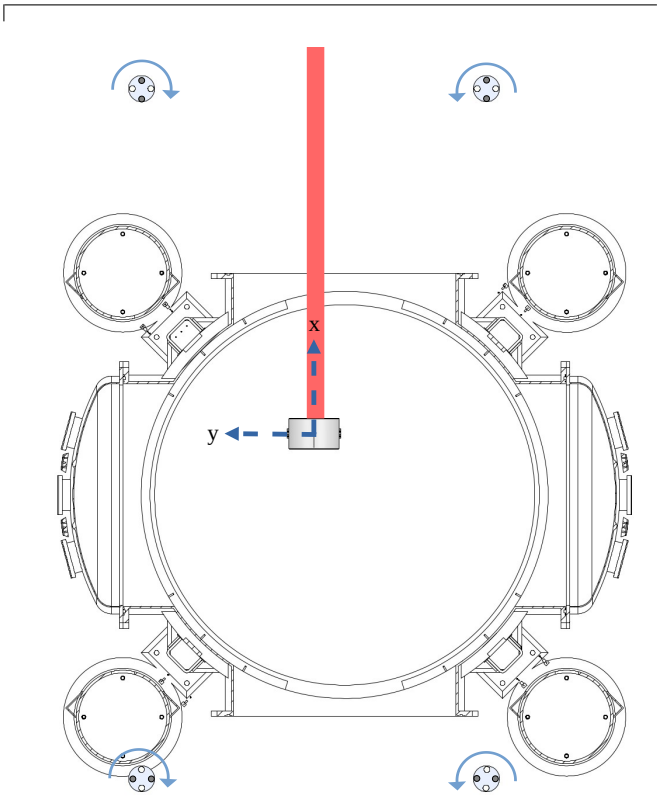

FIG. 2. A rendering of the geometry of the rotor array around the LIGO BSC chamber with the corresponding test mass at the center of our coordinate system and the observatory's main interferometer beam schematically shown in red.

III. ENGINEERING SIMPLICITY

Since the four rotor array produces more acceleration at a given separation than a single rotor, the array can be placed at a larger radius to produce a similar amplitude acceleration on the test mass. This allows the array to be placed well away from the existing infrastructure of the observatories. Here we have chosen a geometry that fits around the LIGO BSC vacuum chamber and seismic

isolation system, as shown in Figure 2. This significantly simplifies the structure that holds the rotors as it does not need to be incorporated into the existing structural components. Additionally, placing the rotors at a larger distance decreases the concerns of damaging the vacuum chamber or isolation in the unlikely scenario that a rotor catastrophically fails.

The use of only quadrupole mass distributions further decreases the safety concerns as the rotors have a smaller radius than similar rotors with multiple multipole mass distributions. This smaller radius decreases the rotor's kinetic energy thus decreasing the likelihood of a catastrophic failure. Due the decreased moment of inertia, a smaller radius also decreases the torques needed to spin the rotor and maintain a fixed rotation speed which loosens the requirements on the drive motors as well as decreases spurious electromagnetic effects caused by the motors and auxiliary electronics.

Parameter	Mean	Uncertainty	Fractional Acceleration Uncertainty
Cylinder Mass	1 kg	0.3 g	3.54×10^{-4}
Cylinder Radius	2 cm	2.5 μm	1.53×10^{-8}
Cylinder Length	5 cm	5 μm	2.74×10^{-8}
Quadrupole Radius	6 cm	5 μm	1.73×10^{-4}
Test Mass*	40 kg	10 g	1.87×10^{-15}
Test Mass Length	200 mm	0.1 mm	4.00×10^{-6}
Test Mass Radius	170 mm	0.05 mm	3.94×10^{-6}
Test Mass Flat Width	327 mm	0.05 mm	1.37×10^{-15}
Rotor Positions	($\pm$ 2.25 m, $\pm$ 1.125 m, 0 m)	(1 mm, 1 mm, 1 mm)	1.05×10^{-3}
Test Mass Position	(0 m, 0 m, 0 m)	(1 cm, 1 cm, 1 cm)	1.34×10^{-4}
Rotor Relative Phase	0°, 90°	1°	1.24×10^{-3}
		Quadrature Sum	1.68×10^{-3}

TABLE II. Individual contributions to the acceleration uncertainty for the parameters of the simulation. *Since the gravitational acceleration is independent of the test mass, this entry represents the numerical precision of the simulation.

IV. PSEUDO PLANE-WAVE NATURE

To verify the performance of such a rotor array, we simulated the system with a finite-element analysis using the *PointGravity* algorithms of the `newt` libraries [22, 23]. This simulation breaks each of the rotor cylinders and the test mass into independent clouds of point masses. The force between each pair of point masses, one from the rotors and the other from the test mass, is calculated. The forces from the individual pairs of point masses is then summed to yield the acceleration in all three directions. We extract only the x-acceleration as this is the sensitive direction of the interferometer. Although not detailed here, the acceleration predictions were cross-checked with the results of an analytical point-mass approximation [21] and an independent numerical integration calculation.

The superposition of the gravitational fields from the four rotors produces an oscillating gravitational acceleration field which at the center of the rectangle is purely in the x-direction and has an amplitude of 101.37 fm/s^2. This amplitude corresponds to a strain of 7.1×10^{-22} at

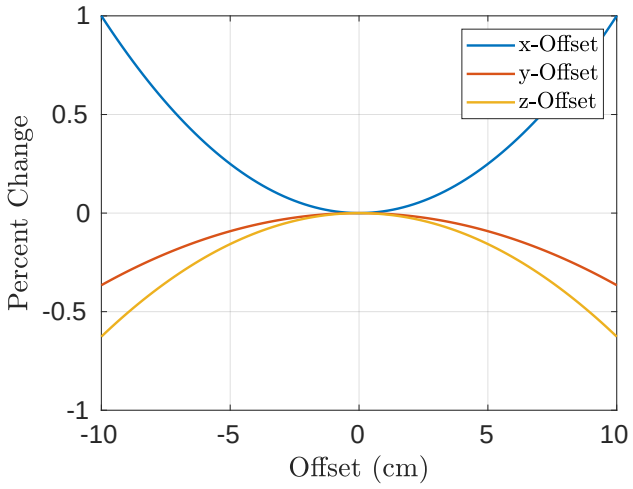

FIG. 3. The percentage change of acceleration amplitude with a test mass offset from the center of the rectangle.

30 Hz for a 4-km long interferometer. Note that although the acceleration amplitude is frequency independent, the strain amplitude will follow $\sim 1/f^2$. The acceleration field changes weakly with deviations from the center of the rectangle (i.e. a pseudo plane-wave). The percentage change in acceleration amplitude verse offset from the center of the rectangle is shown in Figure 3 for offsets in each direction. A relatively large offset of 10 cm in any direction changes the acceleration by $< 1\%$. Additionally, the change in amplitude is well-described by a parabola for small offsets displaying the second-order nature of this effect.

Since the rotor array is in-plane and symmetric about the x-z plane, the rotors apply no net torque on the test mass. If the array is out-of-plane then the test mass would experience a torque about the y-axis. Similarly, if the array is asymmetric it would apply a z-axis torque. Such torques are common in existing gravitational calibrators and can substantially impact the precision of the subsequent calibrations. Note that a different selection of relative rotor phases and rotation directions can apply a net torque on the test mass with no net force. This configuration could provide a novel diagnostic tool for evaluating the interferometer's angular sensitivity and beam spot offsets.

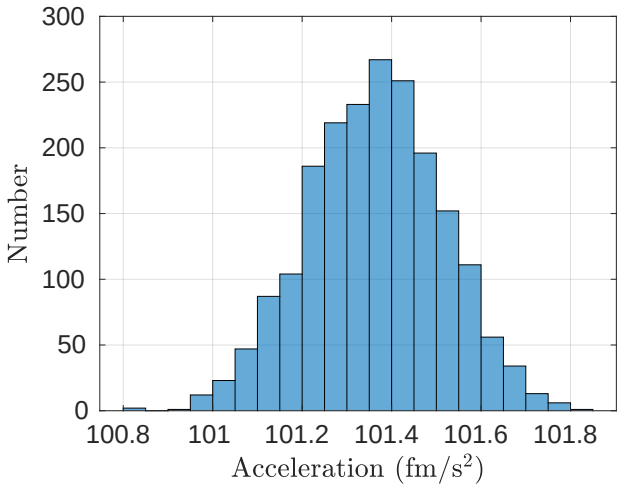

FIG. 4. Distribution of predicted accelerations.

V. NUMERICAL UNCERTAINTY ANALYSIS

The ultimate precision of our four-rotor calibrator depends not only on the test mass offset but all the parameters in Table I. We performed a Monte Carlo simulation of the applied acceleration accounting for the set of parameters which describe the calibrator. We model each parameter as a Gaussian distribution centered on the mean listed in Table I with σ-value equal to the uncertainty. The acceleration of the test mass is then calculated with parameters sampled from these distributions. This is repeated 2000 times to yield a distribution of the gravitational acceleration, shown in Figure 4, which takes into account all non-linearities and degeneracies.

The simulation yields an injected acceleration of $a = 101.37 \pm 0.15$ fm/s^2 (0.15 %) where the central value is the mean and the uncertainty is the 68%-confidence. To assess how each parameter contributes to this total uncertainty, the acceleration uncertainty was recomputed with only one parameter varying. This was then repeated for each parameter to yield the results in Table II. All four rotor positions were simultaneously varied in all three directions and the test mass position was also varied in all three directions.

Table II shows the acceleration uncertainty is strongly dominated by the rotor positions and relative phases with the test mass position contribution being 7-9 times smaller. These contributions may be further reduced with a with higher precision surveying and phase determination than is assumed here.

VI. CONCLUSION

We have described a four-rotor gravitational calibrator that produces a psuedo-plane wave acceleration field. Simulation of the acceleration amplitude uncertainty shows that such a system can achieve an absolute precision of $\sim 0.1\%$. This is approximately an order of magnitude improvement over previously deployed geometries. [21]

ACKNOWLEDGMENTS

Participation from the University of Washington, Seattle, was supported by funding from the NSF under Awards PHY-1607385, PHY-1607391, PHY-1912380, and PHY-1912514.

[1] J. Aasi et al. Advanced LIGO. *Classical and Quantum Gravity*, 32(7):074001, mar 2015. doi:10.1088/0264-9381/32/7/074001. URL `https://doi.org/10.1088%2F0264-9381%2F32%2F7%2F074001`.

[2] F Acernese et al. Advanced Virgo: a second-generation interferometric gravitational wave detector. *Classical and Quantum Gravity*, 32(2):024001, Dec 2014. doi:10.1088/0264-9381/32/2/024001. URL `https://doi.`

org/10.1088%2F0264-9381%2F32%2F2%2F024001.

[3] M Saleem, Javed Rana, V Gayathri, Aditya Vijaykumar, Srashti Goyal, Surabhi Sachdev, Jishnu Suresh, S Sudhagar, Arunava Mukherjee, Gurudatt Gaur, Bangalore Sathyaprakash, Archana Pai, Rana X Adhikari, P Ajith, and Sukanta Bose. The science case for LIGO-india. *Classical and Quantum Gravity*, 39(2):025004, dec 2021. doi:10.1088/1361-6382/ac3b99. URL https://doi.org/10.1088/1361-6382/ac3b99.

[4] T Akutsu, M Ando, K Arai, Y Arai, S Araki, A Araya, N Aritomi, H Asada, Y Aso, S Atsuta, et al. Kagra: 2.5 generation interferometric gravitational wave detector. *NATURE ASTRONOMY*, 3(1):35, 2019.

[5] Rich Abbott, TD Abbott, S Abraham, F Acernese, K Ackley, A Adams, C Adams, RX Adhikari, VB Adya, C Affeldt, et al. Population properties of compact objects from the second LIGO-virgo gravitational-wave transient catalog. *arXiv preprint arXiv:2010.14533*, 2020. URL https://arxiv.org/abs/2010.14533.

[6] BP Abbott, R Abbott, TD Abbott, S Abraham, F Acernese, K Ackley, C Adams, RX Adhikari, VB Adya, C Affeldt, et al. A gravitational-wave measurement of the hubble constant following the second observing run of advanced LIGO and virgo. *The Astrophysical Journal*, 909(2):218, 2021. URL https://iopscience.iop.org/article/10.3847/1538-4357/abdcb7/.

[7] LIGO Scientific Collaboration, Virgo Collaboration, 1M2H Collaboration, Dark Energy Camera GW-EM Collaboration, DES Collaboration, DLT40 Collaboration, Las Cumbres Observatory Collaboration, VINROUGE Collaboration, MASTER Collaboration, et al. A gravitational-wave standard siren measurement of the hubble constant. *Nature*, 551(7678):85–88, 2017. URL https://www.nature.com/articles/nature24471.

[8] Bernard F Schutz. Determining the hubble constant from gravitational wave observations. *Nature*, 323(6086):310–311, 1986.

[9] R Abbott, TD Abbott, S Abraham, F Acernese, K Ackley, A Adams, C Adams, RX Adhikari, VB Adya, C Affeldt, et al. Tests of general relativity with binary black holes from the second LIGO-virgo gravitational-wave transient catalog. *arXiv preprint arXiv:2010.14529*, 2020. URL https://arxiv.org/abs/2010.14529.

[10] S Karki, D Tuyenbayev, S Kandhasamy, BP Abbott, TD Abbott, EH Anders, J Berliner, J Betzwieser, C Cahillane, L Canete, et al. The advanced ligo photon calibrators. *Review of Scientific Instruments*, 87 (11):114503, 2016. URL https://doi.org/10.1063/1.4967303.

[11] D Bhattacharjee, Y Lecoeuche, S Karki, J Betzwieser, V Bossilkov, S Kandhasamy, E Payne, and R L Savage. Fiducial displacements with improved accuracy for the global network of gravitational wave detectors. *Classical and Quantum Gravity*, 38(1):015009, nov 2020. doi: 10.1088/1361-6382/aba9ed. URL https://doi.org/10.1088/1361-6382/aba9ed.

[12] Hiromasa Hirakawa, Kimio Tsubono, and Katsunobu Oide. Dynamical test of the law of gravitation. *Nature*, 283(5743):184–185, 1980. URL https://www.nature.com/articles/283184a0.

[13] Kazuaki Kuroda and Hiromasa Hirakawa. Experimental test of the law of gravitation. *Physical Review D*, 32(2): 342, 1985. URL https://doi.org/10.1103/PhysRevD.32.342.

[14] Norikatsu Mio, Kimio Tsubono, and Hiromasa Hirakawa. Experimental test of the law of gravitation at small distances. *Physical Review D*, 36(8):2321, 1987. URL https://doi.org/10.1103/PhysRevD.36.2321.

[15] Pia Astone, M Bassan, S Bates, R Bizzarri, P Bonifazi, R Cardarelli, G Cavallari, E Coccia, A Degasperis, D De Pedis, et al. Evaluation and preliminary measurement of the interaction of a dynamical gravitational near field with a cryogenic gravitational wave antenna. *Zeitschrift für Physik C Particles and Fields*, 50(1):21–29, 1991. URL https://doi.org/10.1007/BF01558552.

[16] P Astone, M Bassan, R Bizzarri, P Bonifazi, L Brocco, P Carelli, E Coccia, C Cosmelli, A Degasperis, S Frasca, et al. Experimental study of the dynamic newtonian field with a cryogenic gravitational wave antenna. *The European Physical Journal C-Particles and Fields*, 5 (4):651–664, 1998. URL https://doi.org/10.1007/s100529800987.

[17] L Matone, P Raffai, S Márka, R Grossman, P Kalmus, Z Márka, J Rollins, and V Sannibale. Benefits of artificially generated gravity gradients for interferometric gravitational-wave detectors. *Classical and Quantum Gravity*, 24(9):2217–2229, apr 2007. doi: 10.1088/0264-9381/24/9/005. URL https://doi.org/10.1088/0264-9381/24/9/005.

[18] D Estevez, B Lieunard, F Marion, B Mours, L Rolland, and D Verkindt. First tests of a newtonian calibrator on an interferometric gravitational wave detector. *Classical and Quantum Gravity*, 35(23):235009, nov 2018. doi: 10.1088/1361-6382/aae95f. URL https://doi.org/10.1088%2F1361-6382%2Faae95f.

[19] Dimitri Estevez, Benoît Mours, and Thierry Pradier. Newtonian calibrator tests during the virgo o3 data taking. *Classical and Quantum Gravity*, 2021. URL https://iopscience.iop.org/article/10.1088/1361-6382/abe2da.

[20] Yuki Inoue, Sadakazu Haino, Nobuyuki Kanda, Yujiro Ogawa, Toshikazu Suzuki, Takayuki Tomaru, Takahiro Yamanmoto, and Takaaki Yokozawa. Improving the absolute accuracy of the gravitational wave detectors by combining the photon pressure and gravity field calibrators. *Phys. Rev. D*, 98:022005, Jul 2018. doi: 10.1103/PhysRevD.98.022005. URL https://link.aps.org/doi/10.1103/PhysRevD.98.022005.

[21] Michael P. Ross, Timesh Mistry, Laurence Datrier, Jeff Kissel, Krishna Venkateswara, Colin Weller, Kavic Kumar, Charlie Hagedorn, Eric Adelberger, John Lee, Erik Shaw, Patrick Thomas, David Barker, Filiberto Clara, Bubba Gateley, Tyler M. Guidry, Ed Daw, Martin Hendry, and Jens Gundlach. Initial results from the ligo newtonian calibrator. *Phys. Rev. D*, 104:082006, Oct 2021. doi:10.1103/PhysRevD.104.082006. URL https://link.aps.org/doi/10.1103/PhysRevD.104.082006.

[22] Charles A. Hagedorn. *A Sub-Millimeter Parallel-Plate Test of Gravity*. PhD thesis, University of Washington, January 2015.

[23] C Hagedorn and JG Lee. Newt (newtonian eot-wash toolkit). *GitHub*, 2021. URL https://github.com/4kbt/NewtonianEotWashToolkit.